Supplementary Information:

Plasmodium UIS3 sequesters host LC3 to avoid elimination by autophagy in hepatocytes

Eliana Real, Lénia Rodrigues, Ghislain G. Cabal, Francisco J. Enguita, Liliana Mancio-Silva, João Mello-Vieira, Wandy Beatty, Iset M. Vera, Vanessa Zuzarte-Luís, Tiago N. Figueira, Gunnar R. Mair, Maria M. Mota

The Supplementary Information includes:

Supplementary Figure 1. Rescue of *uis3(-)* infectivity.

Supplementary Figure 2. Schematic representation of the *uis3* complementation locus.

Supplementary Figure 3. Specificity of the UIS3-LC3 interaction.

Supplementary Figure 4. Non-canonical LC3 targeting to the PVM.

Supplementary Figure 5. Modelling of the protein-protein interaction between UIS3 and LC3.

Supplementary Figure 6. Model depicting the mechanism of UIS3 protection against host autophagy.

Supplementary Figures 7 - 11. Raw data.

Supplementary Table 1. Plasmids used in this study.

Supplementary Table 2. Primers used for *P. berghei* genotyping.

Supplementary Table 3. Primers used for qRT-PCR

Supplementary Table 4. Primers used for UIS3 mutagenesis.

Supplementary Table 5. Statistical analysis.

Supplementary References

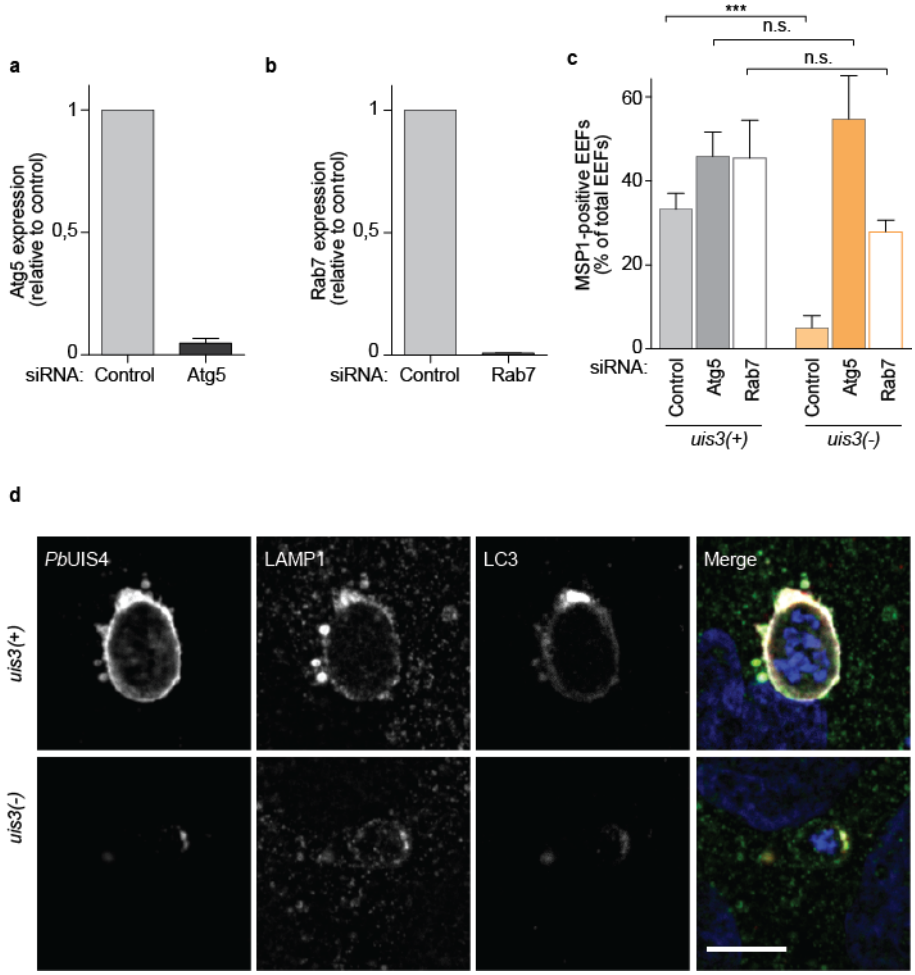

Supplementary Figure 1. Rescue of *uis3(-)* infectivity. a, **b** Expression of Atg5 (a) and Rab7 (b) in HepG2 cells 48 h after siRNA transfection. The mean + SEM of three independent experiments is shown. **c**, Percentage of MSP1-positive parasites quantified by fluorescence microscopy 65 h after infection of HepG2 cells. The bars represent the mean + SEM of pooled replicates from two (Atg5, Rab7) to four (Control) independent experiments. Statistical significance was assessed using non-parametric two-tailed Mann-Whitney test: n.s. $P > 0.05$; ***$P < 0.001$. **d**, Huh7 cells infected with *uis3(+)* or *uis3(-)* parasites (top and bottom panels, respectively) were fixed 24 h after infection and immunostained with anti-UIS4 (white), anti-LAMP1 (green), anti-LC3 (red), and Hoescht (blue). LAMP1 remains outside the lumen of wild-type parasites, but can be observed in the cytosol of dying *uis3(-)* mutants, implying that fusion between the PVM and lysosomes has occurred. The data is representative of at least three independent experiments.

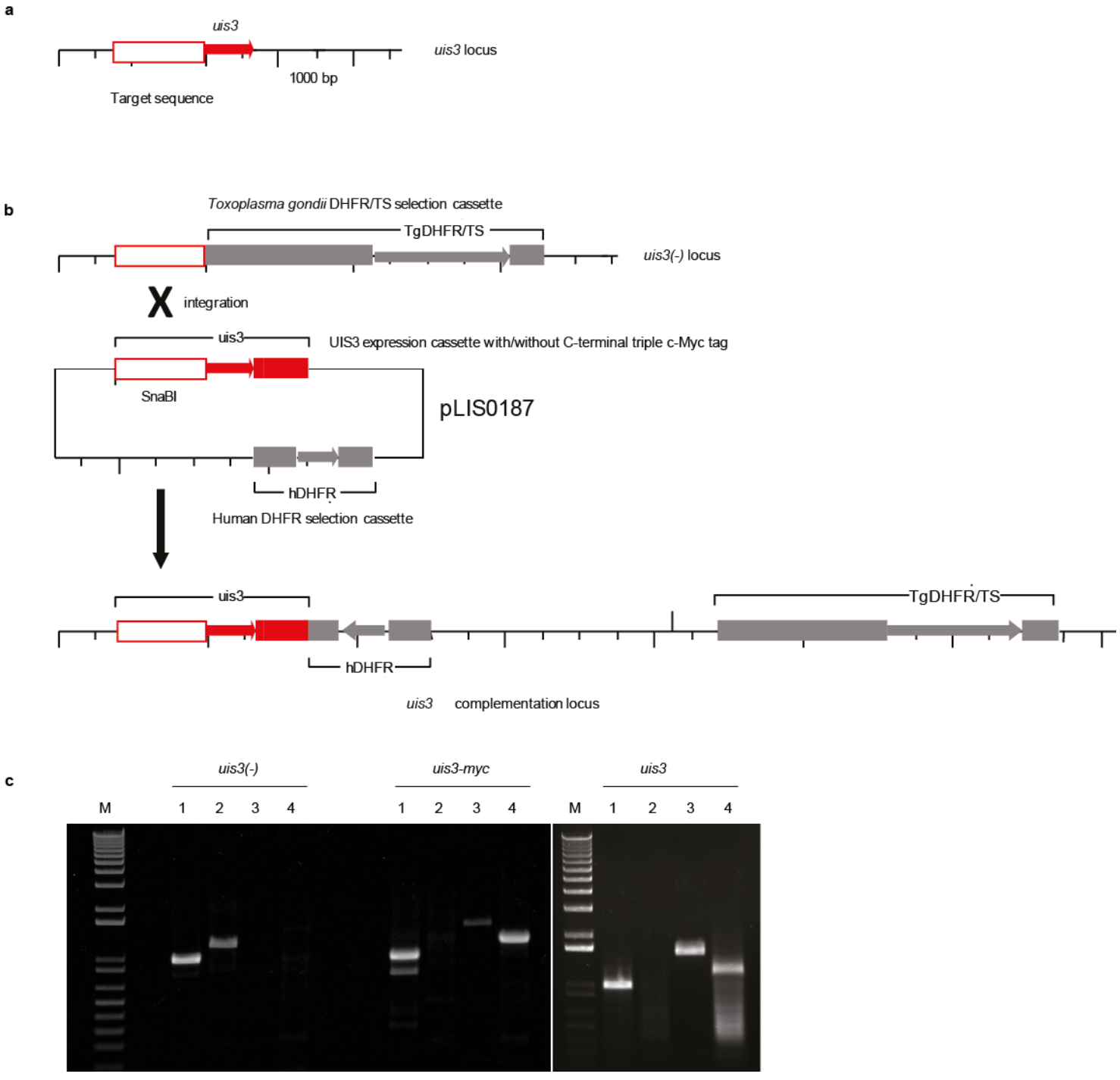

Supplementary Figure 2. Schematic representation of the *uis3* complementation locus. a, *P. berghei uis3* wild-type locus (PBANKA_1400800). **b**, Complementation of the *uis3(-)* locus with *uis3* through single cross-over recombination. The *uis3* complementation locus comprises the *uis3* gene with or without a C-terminal triple c-Myc tag and the human DHFR cassette for drug selection. **c**, PCRs confirming the integration of the *uis3* (with or without *myc*) complementation cassette after transfection of *uis3(-)* parasites and drug selection. The primers used are listed in Table S2. 1: RNA polymerase II (control); 2: *uis3(-)* locus; 3: *uis3* complementation locus 5' integration; 4: *uis3* complementation locus 3' integration.

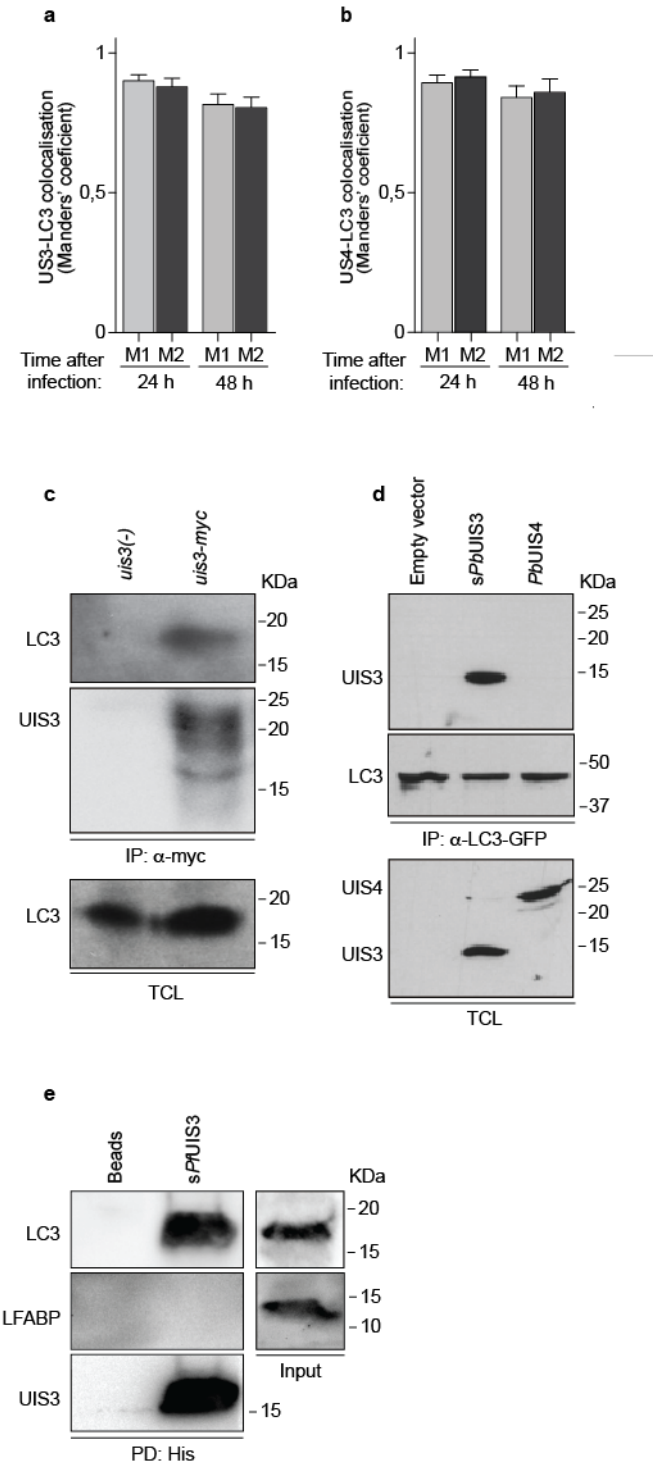
a
US3-LC3 colocalisation (Manders' coeficient)
1
0,5
0
M1 M2 M1 M2
Time after infection:
24 h
48 h
b
US4-LC3 colocalisation (Manders' coeficient)
1
0,5
0
M1 M2 M1 M2
Time after infection:
24 h
48 h
c
uis3(-)
uis3-myc
KDa
LC3
20
15
UIS3
25
20
15
IP: α-myc
LC3
20
15
TCL
d
Empty vector
sPbUIS3
PbUIS4
KDa
UIS3
25
20
15
LC3
50
37
IP: α-LC3-GFP
UIS4
UIS3
25
20
15
TCL
e
Beads
sPfUIS3
KDa
LC3
20
15
LFABP
15
10
UIS3
15
Input
PD: His

Supplementary Figure 3. Specificity of the UIS3-LC3 interaction. a, **b**, Manders' coefficients M1 and M2 (mean + SEM) for colocalisation of UIS3 (a) and UIS4 (b) with LC3. The high Manders' coefficients (values range from 0 to 1) indicate that both parasite proteins colocalise with LC3 to the PVM. Ten randomly selected cells were analysed at each time point. **c**, Lysates of mouse primary hepatocytes infected with *uis3-myc* or *uis3(-) P. berghei* were immunoprecipitated with anti-myc. Analysis of the precipitates was done by western-blot with anti-LC3 and anti-myc antibodies (top and middle panels). Total cell lysates (TCL) were immunoblotted with anti-LC3 (bottom panel). **d**, Whole cell lysates of GFP-LC3 HeLa cells expressing HA-tagged s*Pb*UIS3 or *Pb*UIS4 (extracellular domain) were immunoprecipitated with GFP-Trap beads and analysed by western-blot with anti-HA and anti-LC3 (top and middle panels). UIS3, but not UIS4, co-immunoprecipitated with GFP-LC3. The bottom panel shows the levels of UIS3 and UIS4 in TCL. **e**, Recombinant His-tagged s*Pf*UIS3 was used to pulldown HepG2 total cell extracts. The input and pulldown fractions were probed with antibodies against LC3 (top panels) and L-FABP (middle panels). The pulldown was additionally probed with anti-myc to detect UIS3 (bottom panel). LC3, but not L-FABP, could be detected in the s*Pf*UIS3 pulldown fraction. One immunoblot representative of two independent experiments is shown (c-e).

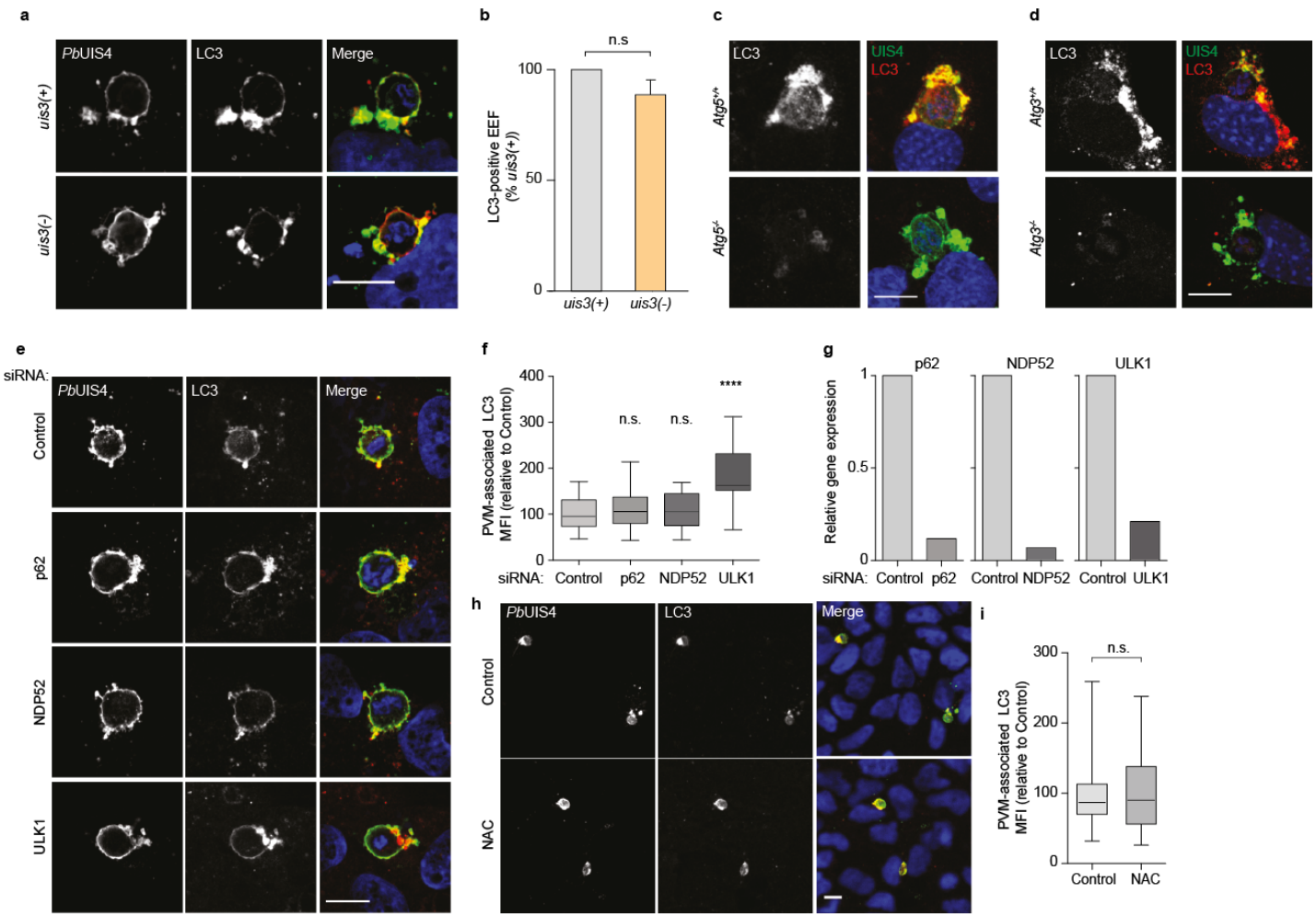

Supplementary Figure 4. Non-canonical LC3 targeting to the PVM. a, Huh7 cells infected with *uis3(+)* (top panel) or *uis3(-)* (bottom panel) parasites were fixed 24 h after infection and imunostained with anti-UIS4 (red), anti-LC3 (green), and Hoechst (blue). Representative images (six independent experiments) are shown. **b**, Number of *uis3(+)* and *uis3(-)* EEFs showing LC3 association 24 h after infection. The bars represent the mean + SEM of > 50 EEFs from six independent experiments, normalised to the average of the *uis3(+)* control. **c**, **d**, Wild-type (top panels) and autophagy-deficient (bottom panels) MEFs were fixed 24 h after infection with *P. berghei* and immunostained as in (a). Representative images (three independent experiments) of infected Atg5 (c) and Atg3 (d) MEFs are shown. **e**, HepG2 cells treated with the indicated siRNAs and infected with wild-type *P. berghei* parasites were fixed 24 h after infection and immunostained as in (a). **f**, Analysis of PVM-associated LC3. The bars represent the box-plot distribution of the mean fluorescence intensity (MFI) measured in the PVM of 17 to 23 EEFs (two independent experiments) and normalized to the control. The whiskers represent maximum and minimum values. **g**, Expression of silenced genes in HepG2 cells 48 h after siRNA transfection. One representative experiment is shown. **h**, Huh7 cells treated with the ROS scavenger N-acetylcysteine (NAC) from 2 h before to 24 h after infection with *P. berghei* parasites were fixed and immunostained as in (a). **i**, MFI of PVM-associated LC3 (box-plot distribution; the whiskers represent maximum and minimum values) in control and NAC-treated Huh7 cells normalized to the average of the control (> 70 EEFs; two independent experiments). Scale bar, 10 μm. Statistical significance was assessed using non-parametric two-tailed Mann-Whitney test: n.s. $P > 0.05$; ****$P < 0.0001$.

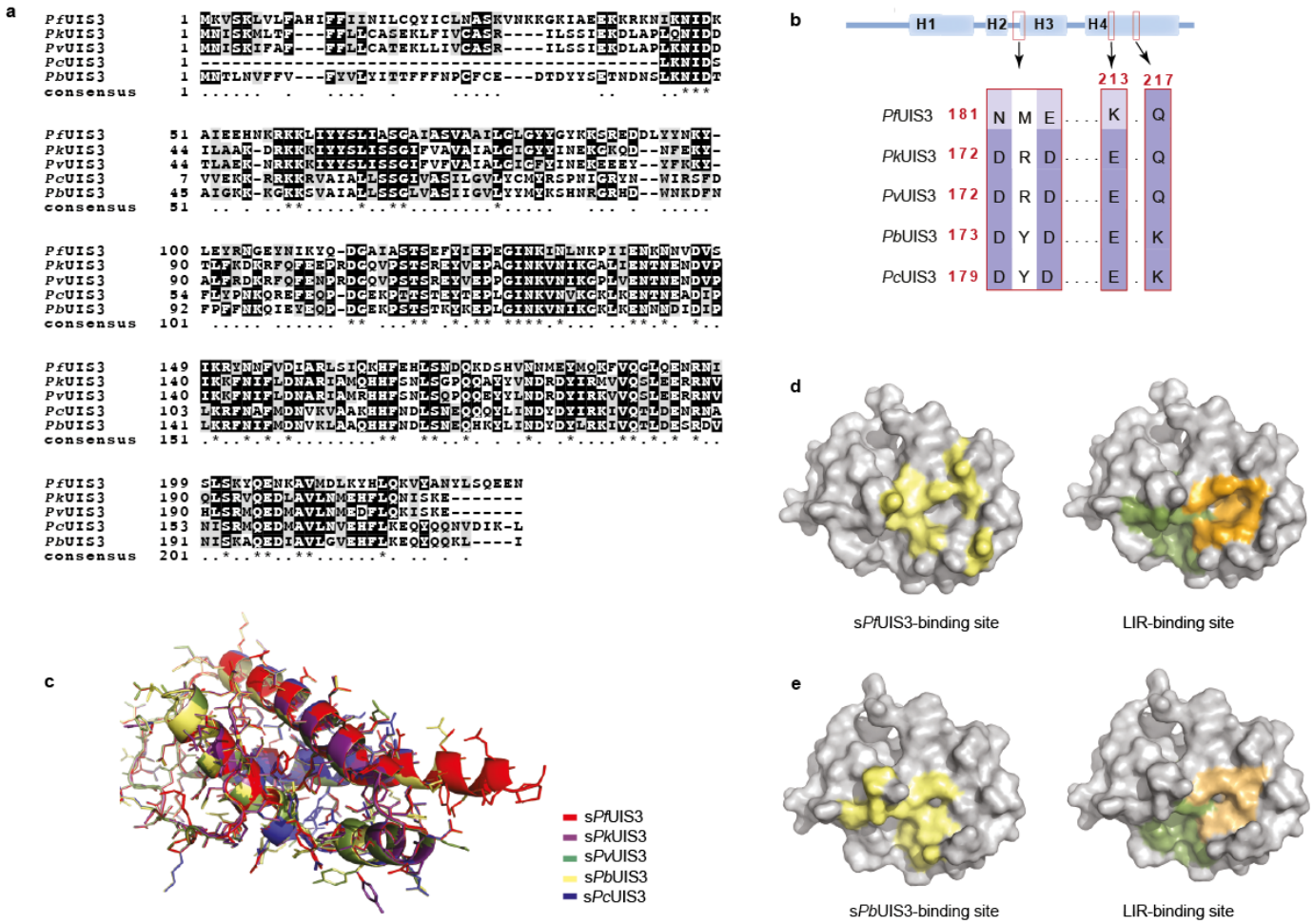

Supplementary Figure 5. Modelling of the protein-protein interaction between UIS3 and LC3. a, ClustalW alignment of the UIS3 sequences from 5 *Plasmodium* species infecting humans, non-human primates, and rodents. Identical (*) and conserved (.) amino acids are shaded in black and grey, respectively. **b**, Secondary structure of the UIS3 soluble domain. The location of the amino acids putatively involved in LC3 binding is shown in red boxes. A sequence alignment (scored and colour-coded according to the BLOSUM62 substitution matrix) underscores the conservation of the amino acids involved in the interaction with LC3, with only one predicted residue (non-coloured) diverging significantly between *Plasmodium* species. **c**, Structure of the soluble domain of *P. falciparum* UIS3 (PDB code: 2VWA) superimposed with homology models of the corresponding UIS3 domains from *P. berghei, P. chabaudi*, *P. knowlesi*, and *P. vivax*. **d**, **e**, Structure of LC3 (PDB code: 2ZJD) with putative UIS3-binding amino acids highlighted in yellow (left) and the two hydrophobic pockets involved in the interaction with canonical LIR motifs coloured green and orange (right). The putative UIS3-binding sites for *P. falciparum* and *P. berghei* UIS3 are depicted in (d) and (e), respectively. Both show partial overlap with the LIR-binding surface.

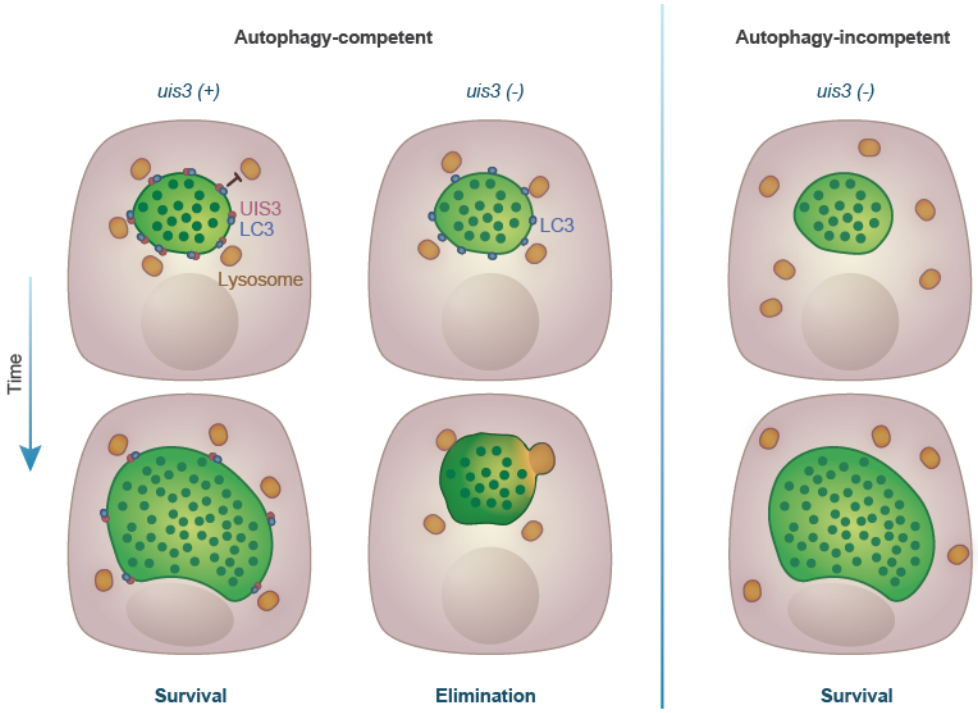

Supplementary Figure 6. Model depicting the mechanism of UIS3 protection against host autophagy. UIS3 interacts with LC3 on the PVM of liver stage *Plasmodium*, blocking the autophagic flux. In this way, wild-type, but not *uis3(-)* parasites avoid LC3-dependent fusion with host lysosomes (inhibition depicted as ⊥). *uis3(-)* parasites become fully viable and infectious when the autophagy pathway of the host cell is compromised.

Supplementary Figures 7-11. Raw data

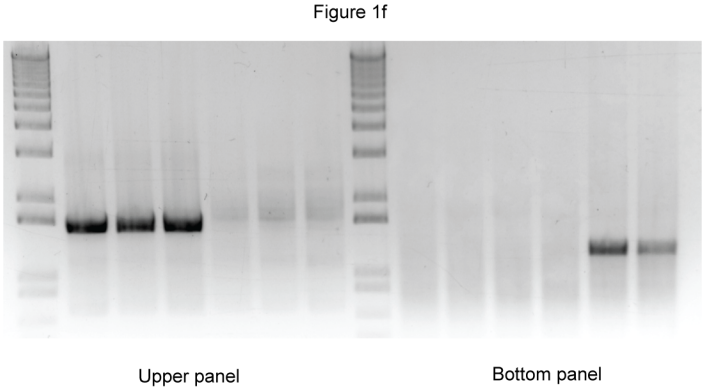

Supplementary Figure 7. Raw data of Figure 1f. Image acquired using a ChemiDoc imaging system. M, 1 Kb DNA ladder.

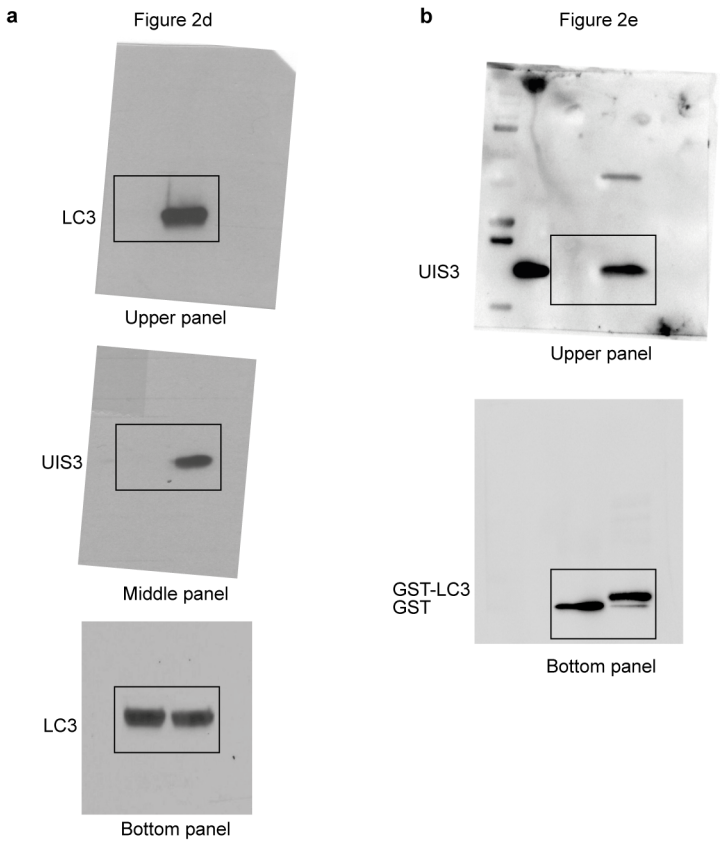

Supplementary Figure 8. a, Raw data of Figure 2d. **b,** Raw data of Figure 2e. The boxes show where the images were cropped to produce the main figure.

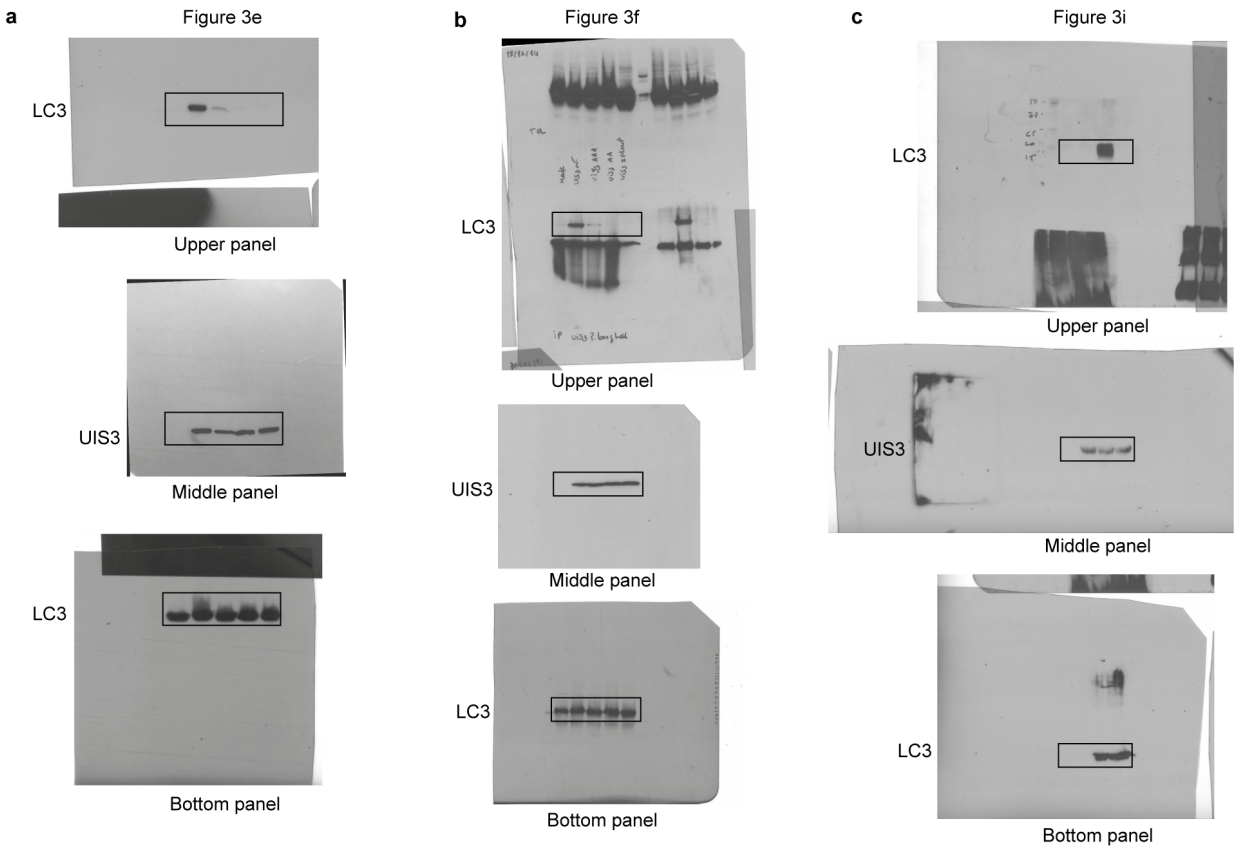

Supplementary Figure 9. **a**, Raw data of Figure 3e. **b,** Raw data of Figure 3f. **c,** Raw data of Figure 3i. The boxes show where the images were cropped to produce the main figure.

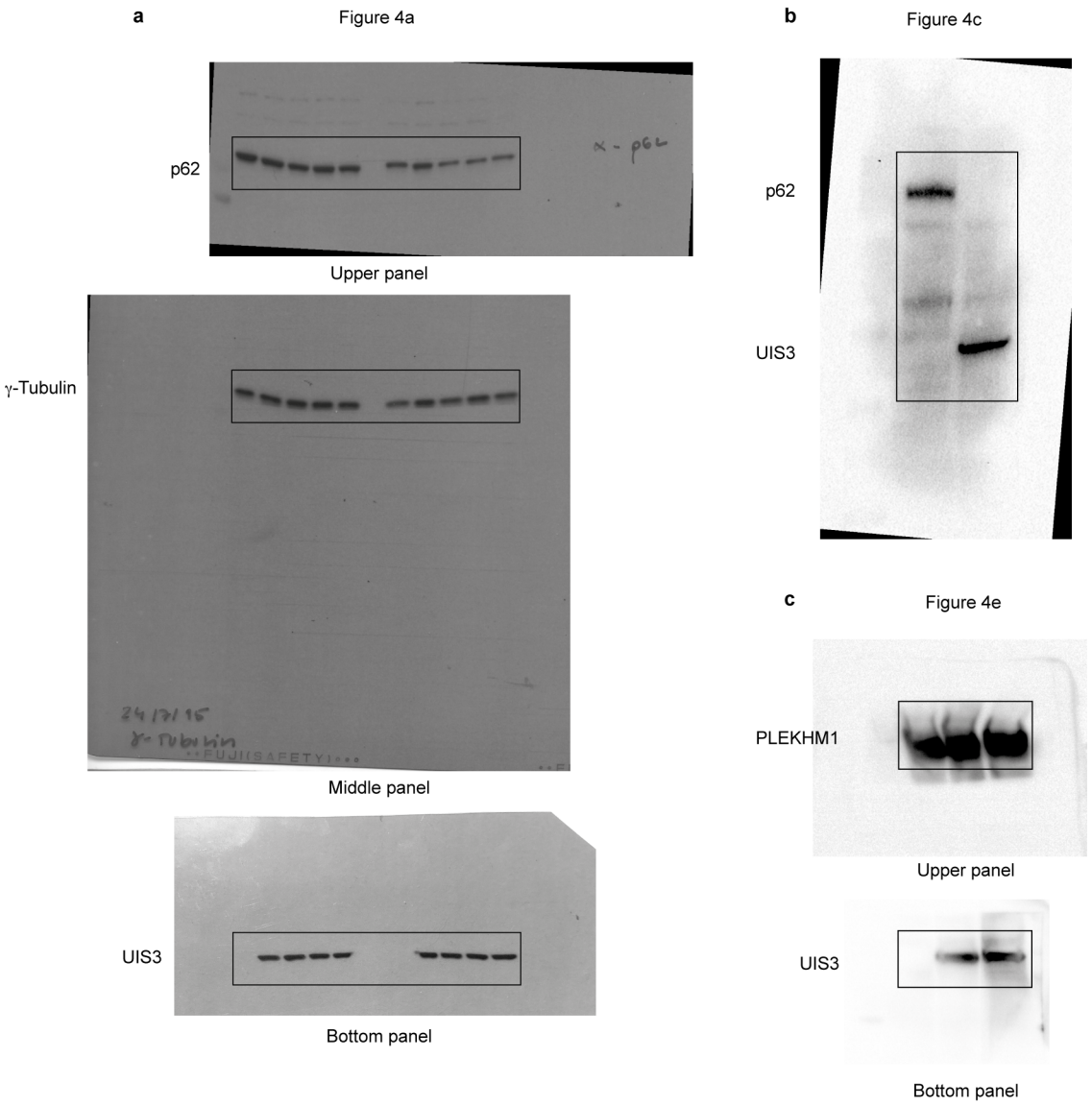

Supplementary Figure 10. **a**, Raw data of Figure 4a. **b,** Raw data of Figure 4c. **c,** Raw data of Figure 4e. (b, c) Images acquired using a ChemiDoc imaging system. The boxes show where the images were cropped to produce the main figure.

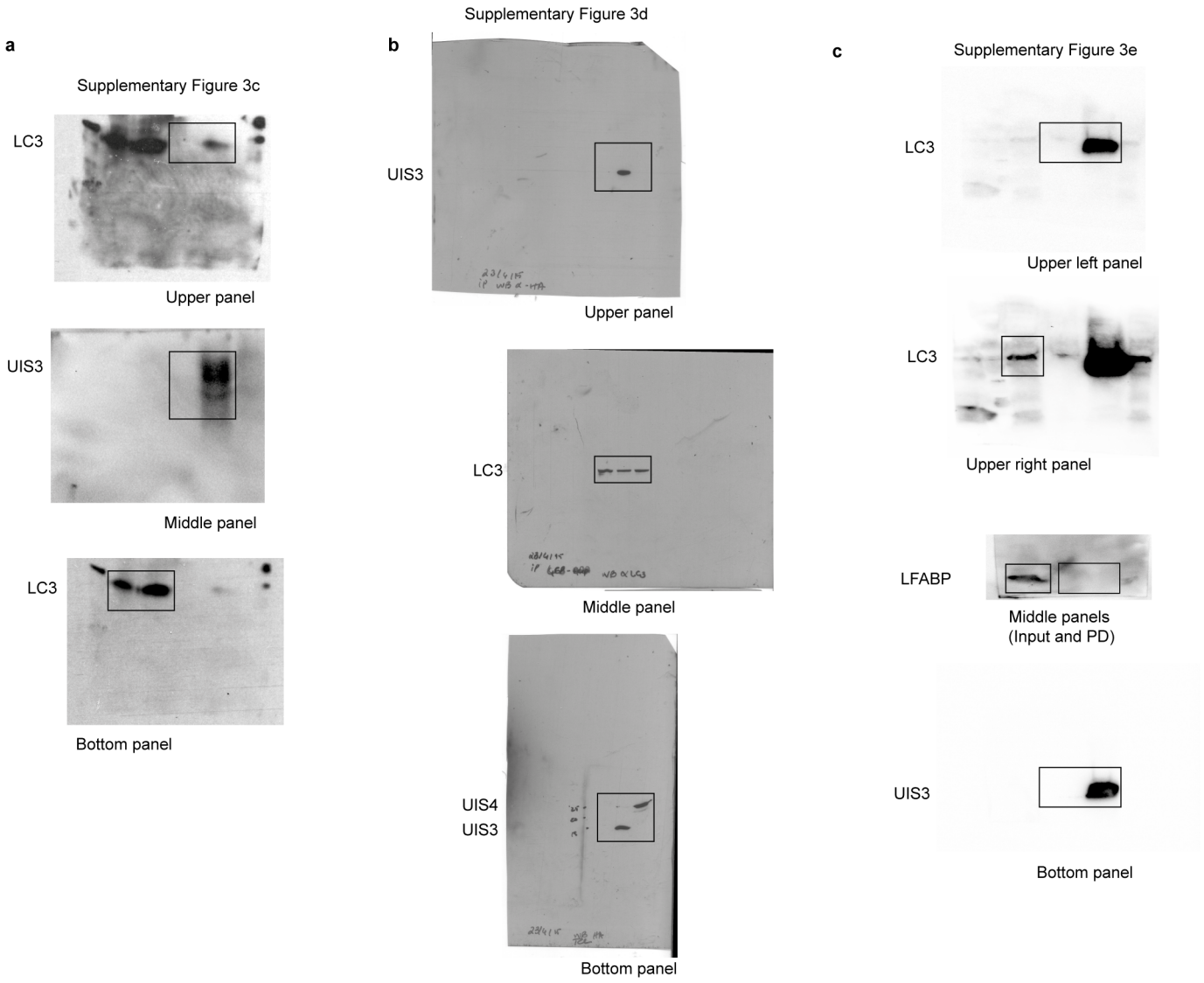

Supplementary Figure 11. a, Raw data of Supplementary Figure 3c. **b,** Raw data of Supplementary Figure 3d. Note that the top and bottom images shown in (a) correspond to the same gel, revealed using different exposure times. In our opinion, the input and pulldown bands are not directly comparable, since the amount of total protein varies between the two samples. Therefore, even though on this occasion both samples appear on the same gel, the exposure conditions were optimized for each sample separately. Similarly, the top two images in (c) also correspond to the same gel, and the exposure conditions were also optimized for each sample (input and pulldown) separately. **c,** Raw data of Supplementary Figure 3e. (a, c) Images acquired using a ChemiDoc imaging system The boxes show where the images were cropped to produce the main figure.

Supplementary Tables

Supplementary Table 1. Plasmids used in this study

Plasmid/Tag	Gene/Mutations	Reference
pCMV-MYC-s*Pb*UIS3^{WT}	*P. berghei* soluble UIS3	This study
pCMV-MYC-s*Pb*UIS3^{Mut1}	*P. berghei* soluble UIS3 D173A, Y174A, D175A	This study
pCMV-MYC-s*Pb*UIS3^{Mut2}	*P. berghei* soluble UIS3 E205A, K209A	This study
pCMV-MYC-s*Pb*UIS3^{Mut3}	*P. berghei* soluble UIS3 D173A, Y174A, D175A, E205A, K209A	This study
pCMV-MYC-s*Pf*UIS3^{WT}	*P. falciparum* soluble UIS3	This study
pCMV-MYC-s*Pf*UIS3^{Mut1}	*P. falciparum* soluble UIS3 N181A, M182A, E183A	This study
pCMV-MYC-s*Pf*UIS3^{Mut2}	*P. falciparum* soluble UIS3 K213A, Q217A	This study
pCMV-MYC-s*Pf*UIS3^{Mut3}	*P. falciparum* soluble UIS3 N181A, M182A, E183A, K213A, Q217A	This study
pCMV-HA-s*Pb*UIS3	*P. berghei* soluble UIS3	This study
pCMV-HA-*Pb*UIS4	*P. berghei* UIS4 aa 100-220	This study
pCMV-HA-LC3^{WT}	Human LC3B	This study
pCMV-HA-LC3^{Mut}	Human LC3B R11A, K49A, T50A, K51A, F52A, L53A	This study
pETM30-LC3B (GST-His6 fusion)	Human LC3B	Supplementary Reference 1
pET28a-UIS3 (His6 fusion)	*P. falciparum* soluble UIS3	This study
pET49b	GST-His6	Novagen
pEGFP-PLEKHM1	Human PLEKHM1	Reference 46
MP5-Luc-p62 (*Renilla* luciferase fusion)	Human p62	Supplementary Reference 1
pCMV-MYC-Luc-s*Pf*UIS3 ^{WT} (*Renilla* luciferase fusion)	*P. falciparum* soluble UIS3	This study

pCMV-MYC-Luc-s*Pf*UIS3 ^{Mut1} (*Renilla* luciferase fusion)	*P. falciparum* soluble UIS3 N181A, M182A, E183A	This study
pCMV-MYC-Luc-s*Pf*UIS3 ^{Mut4} (*Renilla* luciferase fusion)	*P. falciparum* soluble UIS3 N181A	This study
pCMV-MYC-Luc-s*Pf*UIS3 ^{Mut5} (*Renilla* luciferase fusion)	*P. falciparum* soluble UIS3 M182A	This study
pCMV-MYC-Luc-s*Pf*UIS3 ^{Mut6} (*Renilla* luciferase fusion)	*P. falciparum* soluble UIS3 E183A	This study
pCMV-MYC-Luc-s*Pf*UIS3 ^{Mut7} (*Renilla* luciferase fusion)	*P. falciparum* soluble UIS3 K213A	This study
pCMV-MYC-Luc-s*Pf*UIS3 ^{Mut8} (*Renilla* luciferase fusion)	*P. falciparum* soluble UIS3 Q217A	This study

Supplementary Table 2. Primers used for *P. berghei* genotyping

PCR reaction	**Primers pairs**
5’ integration	5’TAATTGATCAACATAATG3’; 5’GTTCTTTATATTTTGTACTAGTGCTTGGC3’
3’ integration	5’ GTTTTCCCAGTCACGACGTTG 3’; 5’ATTGTTGACCTGCAGGCATG3’
uis3(-) locus	5’TAATTGATCAACATAATG3’; 5’ATTGTTGACCTGCAGGCATG3’
RNA polymerase II (control)	5’AAAGAATTCTGATGGTTTACAATCACC3’; 5’AAAGCGGCCGCTTTCTTCCTGCATCTCCTC3’

Supplementary Table 3. Primers used for qRT-PCR

PCR reaction	Primers pairs
Atg5	5’AGACCTTCTGCACTGTCCAT3’; 5’CGATTGATGGCCCAAAACTGG3’
Rab7	5’ GATGTCTTCCCGACTCCAGA3’; 5’TCCGTTTAGTCTCCTCCTCG3’
SQSTM1/p62	5’TTCTTTTCCCTCCGTGCTC3’; 5’GGATCCGAGTGTGAATTTCC3’
NDP52	5’GCAAGACAGCTGATGTGGG3’; 5’CACTCTGCCCTGTTGCTGT3’
ULK1	5’CGTTGCAGTACTCCATAACCAG3’; 5’GGGGAAGGAAATCAAAATCC3’
HPRT1	5’TTTGCTGACCTGCTGGATTAC3’; 5’CAAGACATTCTTTCCAGTTAAAGTTG3’

Supplementary Table 4. Primers used for UIS3 mutagenesis

PCR reaction	Primers pairs
s*Pf*UIS3^{Mut4}	5’ TTTCTGCATGTACTCCATGGCGTTCACGTGGCTGTCTTTC 3’; 5’ GAAAGACAGCCACGTGAACGCCATGGAGTACATGCAGAAA 3’
s*Pf*UIS3^{Mut5}	5’ GAATTTCTGCATGTACTCCGCGTTGTTCACGTGGCTGTCT 3’; 5’AGACAGCCACGTGAACAACGCGGAGTACATGCAGAAATTC 3’
s*Pf*UIS3^{Mut6}	5’CGAATTTCTGCATGTACGCCATGTTGTTCACGTGG 3’; 5’ CCACGTGAACAACATGGCGTACATGCAGAAATTCG 3’
s*Pf*UIS3^{Mut7}	5’CTTCTGCAGATGGTACGCCAGGTCCATCACGGCC 3’; 5’ GGCCGTGATGGACCTGGCGTACCATCTGCAGAAG 3’
s*Pf*UIS3^{Mut8}	5’TAGTTGGCGTACACCTTCGCCAGATGGTACTTCAGGTC 3’; 5’GACCTGAAGTACCATCTGGCGAAGGTGTACGCCAACTA 3’

Supplementary Table 5. Statistical analysis

Fig. 1c (n=2-4)	P value	Test
Control siRNA *uis3(+)*	< 0,0001	Non-parametric two-tailed Mann-Whitney
Control siRNA *uis3(-)*		
Atg5 siRNA *uis3(+)*	0,0714	
Atg5 siRNA *uis3(-)*		
Rab7 siRNA *uis3(+)*	0,0547	
Rab7 siRNA *uis3(-)*		

Fig. 1g (n=5)	P value	Test
MEFS Atg3$^{+/+}$ *uis3(+)*	0,0002	Non-parametric two-tailed Mann-Whitney
MEFS Atg3$^{+/+}$ *uis3(-)*		
MEFS Atg3$^{-/-}$ *uis3(+)*	0,4277	
MEFS Atg3$^{-/-}$ *uis3(-)*		
MEFS Atg5$^{+/+}$ *uis3(+)*	0,0016	
MEFS Atg5$^{+/+}$ *uis3(-)*		
MEFS Atg5$^{-/-}$ *uis3(+)*	0,9399	
MEFS Atg5$^{-/-}$ *uis3(-)*		
MEFS Atg7$^{+/+}$ *uis3(+)*	< 0,0001	Non-parametric two-tailed Mann-Whitney
MEFS Atg7$^{+/+}$ *uis3(-)*		
MEFS Atg7$^{-/-}$ *uis3(+)*	0,6604	
MEFS Atg7$^{-/-}$ *uis3(-)*		

Fig. 1h (n=3)	P value	Test
Control *uis3(+)*	<0,0001	Non-parametric two-tailed Mann-Whitney
Control *uis3(-)*		
Control *uis3(+)*	0,3020	
CQ *uis3(+)*		
Control *uis3(+)*	0,3421	
CQ *uis3(-)*		
Control *uis3(-)*	0,0003	
CQ *uis3(-)*		

Fig. 3g (n=2)	P value	Test
s*Pf*UIS3^{WT}	<0.0001	Unpaired two-tailed *t* Test
s*Pf*UIS3^{Mut1}		
s*Pf*UIS3^{WT}	0,0081	
s*Pf*UIS3^{Mut4}		
s*Pf*UIS3^{WT}	0,0028	
s*Pf*UIS3^{Mut5}		
s*Pf*UIS3^{WT}	0,0088	
s*Pf*UIS3^{Mut6}		
s*Pf*UIS3^{WT}	0,0012	
s*Pf*UIS3^{Mut7}		
s*Pf*UIS3^{WT}	0,0264	
s*Pf*UIS3^{Mut8}		

Fig. 4b (n=5)	P value	Test
Empty vector control	< 0,0001	Unpaired two-tailed *t* test
Empty vector aa starvation		
UIS3 ^{WT} control	0,2334	
UIS3 ^{WT} aa starvation		
UIS3 ^{Mut1} control	0,0001	
UIS3 ^{Mut1} aa starvation		
UIS3 ^{Mut2} control	< 0,0001	
UIS3 ^{Mut2} aa starvation		
UIS3 ^{Mut3} control	< 0,0001	
UIS3 ^{Mut3} aa starvation		

Fig. 4d (n=2-3)	P value	Test
p62	< 0,0001	Two-way ANOVA
s*Pf*UIS3		

Fig. 4e GFP Fluorescence (n=3)	P value	Test
GFP-PLEKHM1	< 0,0001	Unpaired two-tailed *t* test
GFP-PLEKHM1 + s*Pf*UIS3^{WT}		
GFP-PLEKHM1	0,0828	
GFP-PLEKHM1 + s*Pf*UIS3^{Mut1}		
GFP-PLEKHM1 + s*Pf*UIS3^{WT}	0,0107	
GFP-PLEKHM1 + s*Pf*UIS3^{Mut1}		

Fig. 4e s*Pf*UIS3 Luciferase activity (n=3)	P value	Test
GFP-PLEKHM1 + s*Pf*UIS3^{WT}	< 0,0001	Unpaired two-tailed *t* test
GFP-PLEKHM1 + s*Pf*UIS3^{Mut1}		

Extended data Fig. 1c (n=2-4)	P value	Test
Control siRNA *uis3(+)*	0,0006	Non-parametric two-tailed Mann-Whitney
Control siRNA *uis3(-)*		
Atg5 siRNA *uis3(+)*	0,4534	
Atg5 siRNA *uis3(-)*		
Rab7 siRNA *uis3(+)*	0,1199	
Rab7 siRNA *uis3(-)*		

Extended Data Fig. 4b (n=6)	P value	Test
uis3(+)	0,0740	Non-parametric two-tailed Mann-Whitney
uis3(-)		

Extended Data Fig. 4f (n=17-23)	P value	Test
Control siRNA	0,3931	Non-parametric two-tailed Mann-Whitney
p62 siRNA		
Control siRNA	0,7397	
NDP52 siRNA		
Control siRNA	< 0,0001	
ULK1 siRNA		

Extended Data Fig. 4i (n=71-75)	P value	Test
Control	0,9220	Non-parametric two-tailed Mann-Whitney
NAC		

Supplementary References

1. von Muhlinen, N. *et al.* LC3C, bound selectively by a noncanonical LIR motif in NDP52, is required for antibacterial autophagy. *Mol. Cell* **48,** 329–42 (2012).